VAMP5 promotes Fcγ receptor-mediated phagocytosis and regulates phagosome maturation in macrophages

Chiye Sakurai, Natsumi Yamashita, Kento Azuma, and Kiyotaka Hatsuzawa*
Division of Molecular Biology, School of Life Sciences, Faculty of Medicine, Tottori University, Yonago, Tottori 683-8503, Japan

ABSTRACT **Phagosome formation and maturation reportedly occur via sequential membrane fusion events mediated by synaptosomal-associated protein of 23 kDa (SNAP23), a plasma membrane-localized soluble *N*-ethylmaleimide-sensitive factor attachment protein receptor (SNARE) family. Vesicle-associated membrane protein 5 (VAMP5), also a plasmalemma SNARE, interacts with SNAP23; however, its precise function in phagocytosis in macrophages remains elusive. To elucidate this aspect, we investigated the characteristics of macrophages in the presence of VAMP5 overexpression or knockdown and found that VAMP5 participates in Fcγ receptor-mediated phagosome formation, although not directly in phagosome maturation. Overexpressed VAMP5 was localized to the early phagosomal membrane but no longer localized to the lysosomal-associated membrane protein 1-positive maturing phagosomal membrane. Analyses using compound-based selective inhibitors demonstrated that VAMP5 dissociation from early phagosomes occurs in a clathrin- and dynamin-dependent manner and is indispensable for SNAP23 function in subsequent membrane fusion during phagosome maturation. Accordingly, to the best of our knowledge, we demonstrate, for the first time, that VAMP5 exerts an immunologically critical function during phagosome formation and maturation via SNARE-based membrane trafficking in macrophages.**

SIGNIFICANCE STATEMENT

- FcR-mediated phagocytosis reportedly occurs via sequential membrane fusion mediated by SNAP23, a plasmalemmal SNARE. VAMP5 is a SNARE that interacts with SNAP23; however, whether VAMP5 functions in phagocytosis remains unknown.
- Using macrophages overexpressing or knocking down VAMP5, VAMP5 was found to regulate phagocytosis. Furthermore, VAMP5 dissociation from phagosomes was found to be dependent on clathrin and dynamin activity and was crucial for subsequent phagosome maturation.
- These findings contribute to a better understanding of the regulatory mechanisms of phagocytosis, implicating a critical function for VAMP5 in phagocytosis via SNARE-based membrane trafficking for immunological defense in macrophages.

Monitoring Editor
Sergio Grinstein
Hospital for Sick Children

Received: May 1, 2023
Revised: Jan 12, 2024
Accepted: Jan 18, 2024

Cross-Validation

New Hypothesis

New Materials

This article was published online ahead of print in MBoC in Press (http://www.molbiolcell.org/cgi/doi/10.1091/mbc.E23-04-0149) on January 24, 2024.

*Address correspondence to: Kiyotaka Hatsuzawa (hatsu@tottori-u.ac.jp)

Abbreviations used: AP, clathrin adaptor protein; α-SNAP, α-soluble NSF attachment protein; ER, endoplasmic reticulum; FcR, Fcγ receptor; FRET, Förster resonance energy transfer; LAMP1, lysosomal-associated membrane protein 1; MiTMAB, myristyl trimethyl ammonium bromide; NSF, *N*-ethylmaleimide-sensitive factor; RB, rhodamine B; SNAP23, synaptosomal-associated protein of 23 kDa; SNARE, soluble *N*-ethylmaleimide-sensitive factor attachment protein receptor; stx, syntaxin; TR, Texas Red; VAMP5, vesicle-associated membrane protein 5; WT, wild type.

INTRODUCTION

Phagocytosis is the endocytosis of particles larger than 0.5 μm, typically mediated by macrophages and immature dendritic cells. It is a crucial process that kills and degrades pathogens for host defense and also clears apoptotic and necrotic cells for tissue homeostasis (Boulais *et al.*, 2010; Underhill and Goodridge, 2012). Phagocytosis is triggered by cell surface receptors that recognize target particle components, such as Fcγ receptors for immunoglobulins, complement receptors, and pattern-recognition receptors for pathogen-associated molecular patterns (Pauwels *et al.*, 2017). The newly formed phagosome progressively matures through a membrane fusion/fission series with endocytic compartments. Phagosomes gradually mature with the acquisition of microbicidal reactive oxygen species, an acidic milieu, and lysosomal hydrolases, ultimately becoming phagolysosomes (Pauwels *et al.*, 2017; Fountain *et al.*, 2021; Nguyen and Yates, 2021). During phagocytosis, the dynamin superfamily of GTPases mediates the scission of vesicles from the plasma membrane and phagosome. Dynamin-2/DYN-1/DymA (mammalian/*Caenorhabditis elegans*/*Dictyostelium discoideum* homolog proteins) and clathrin reportedly participate not only in pseudopod extension (with actin polymerization) and phagosome closure during phagosome formation but also in the early stages of phagosome maturation (Gold *et al.*, 1999; Kinchen *et al.*, 2008; Gopaldass *et al.*, 2012; Chen *et al.*, 2013; Marie-Anais *et al.*, 2016). Phagolysosomes are fragmented by vesiculation, tubulation, and constriction through the function of the actin and microtubule cytoskeletons, clathrin, BLOC-1-related complex (BORC), and ARL8, eventually reforming into lysosomes over time (Lancaster *et al.*, 2021; Fazeli *et al.*, 2023). This process is called "phagosome/phagolysosome resolution" (Levin *et al.*, 2016; Fountain *et al.*, 2021). It is known that phagosome maturation and resolution during phagocytosis are complex processes involving the fusion and (or) fission of various membrane types; however, the mechanisms underlying SNARE-mediated fusion remains largely elusive.

Similar to several membrane fusion events in vesicular transport between the intracellular organelles, the fusion of the plasma membrane or phagosomes to vesicles derived from the secretory and endocytic organelles, which occurs during phagocytosis, depends on soluble *N*-ethylmaleimide-sensitive fusion factor attachment protein receptors (SNAREs; Stow *et al.*, 2006; Hatsuzawa and Sakurai, 2020; Nguyen and Yates, 2021). Membrane fusion is accomplished via the formation of the SNARE complex using coiled-coil bundles of four helices. Three Q-SNARE motifs are derived from the syntaxin and SNAP25 families (Q-SNARE proteins are further classified into Qa- and Qbc-SNARE subfamilies). One R-SNARE motif is derived from the vesicle-associated membrane protein (VAMP, also called synaptobrevin) family. Post-fusion, the SNARE complex on the same membrane is disassembled via a cooperative reaction of *N*-ethylmaleimide-sensitive factor (NSF) with α-soluble NSF attachment protein (α-SNAP) to be recycled into the subsequent round of fusion (Fasshauer *et al.*, 1998; Jahn and Scheller, 2006; Hong and Lev, 2014). Phagosome formation in macrophages requires the plasma membrane-localized SNARE proteins SNAP23 (synaptosomal-associated protein of 23 kDa; a Qbc-SNARE) and syntaxin 4 (a Qa-SNARE; Murray *et al.*, 2005; Stow *et al.*, 2006; Sakurai *et al.*, 2012). Primarily, SNAP23 also regulates the phagosome maturation process in combination with VAMP3 (recycling endosome-localized), VAMP8 (recycling endosome- or partly lysosome-localized), and VAMP7 (lysosome-localized) belonging to R-SNARE subfamily (Sakurai *et al.*, 2012; Nair-Gupta *et al.*, 2014). During Fcγ receptor (FcR)-mediated phagocytosis in interferon-γ-activated macrophages, SNAP23 phosphorylated at Ser95 negatively regulates phagosome maturation (Sakurai *et al.*, 2018; Hatsuzawa and Sakurai, 2020). Conversely, the ultimate dissociation and recycling mechanisms of SNAP23-containing SNARE complexes on the phagosomal membrane remain unknown.

Using immunoprecipitation experiments with macrophage cell lysates, we have shown that SNAP23 interacts with various SNAREs, including VAMPs such as VAMP3, VAMP4, VAMP5, VAMP7, and VAMP8. Moreover, using an intramolecular Förster resonance energy transfer (FRET) probe of SNAP23, we found that VAMP5 interacts with SNAP23 at the plasma membrane in vivo (Sakurai *et al.*, 2012, 2018). Unlike other VAMPs, VAMP5 was primarily distributed on the plasma membrane in mouse C2C12 myoblasts and skeletal and cardiac muscle cells (Zeng *et al.*, 1998; Takahashi *et al.*, 2013). VAMP5 was found in muscle, kidney, lung, liver, spleen, and radial glial (Müller) cells (Takahashi *et al.*, 2013). Analysis of VAMP5 knockout mice revealed average fetal growth at embryonic d 16.5, but a low birth rate, along with abnormalities in the urinary and respiratory systems (Ikezawa *et al.*, 2018). However, the molecular mechanisms of membrane fusion involving VAMP5 are largely unknown.

In the current study, we aimed to elucidate the molecular mechanisms underlying the function of VAMP5 and its relationship with partner SNARE protein(s) during FcR-mediated phagocytosis in macrophages. To the best of our knowledge, we provide the first critical function of VAMP5 in phagosome formation and maturation via SNARE-based membrane trafficking for immunological defense in macrophages.

RESULTS

Overexpression of Myc-tagged VAMP5 in macrophages enhances FcR-mediated phagocytosis but not phagosome-lysosome fusion

To explore the function of VAMP5 in FcR-mediated phagocytosis, we established the murine macrophage-like cell line J774 overexpressing Myc-tagged VAMP5 (J774/Myc-VAMP5). The expression level of Myc-VAMP5 against endogenous VAMP5 was considerably higher (more than two-fold) than that of Myc-SNAP23 against endogenous SNAP23 (Figure 1A). Similar to Myc-SNAP23, Myc-VAMP5 was predominately localized to the plasma membrane and partly to the endomembranes (Figure 1B). Upon exposure of J774/Myc-VAMP5 cells to IgG-opsonized zymosan particles labeled with Texas Red (IgG-TR-zymosan), Myc-VAMP5 could also be observed on the phagosomal membrane (Figure 1B). We next examined the effects of Myc-VAMP5 overexpression on the phagocytosis efficiency in J774/Myc-VAMP5 cells. We found that J774/Myc-VAMP5 cells exhibited a significantly enhanced phagocytosis efficiency compared with the control J774 cells expressing the Myc-tag alone, although there was no difference in the association efficiency with IgG-TR-zymosan between each cell line (Figure 1C). Moreover, J774/Myc-SNAP23 cells demonstrated an increased phagocytosis efficiency. We next investigated phagosome–lysosome fusion efficiency in J774/Myc-VAMP5 cells by labeling lysosomes with rhodamine B (RB)-conjugated dextran as a fluid-phase marker. The labeling efficiency of lysosomes by steady-state uptake of RB-dextran did not differ between examined cells (Figure 1D, left). The percentage of RB-dextran-positive phagosomes was significantly enhanced in J774/Myc-SNAP23 cells; however, J774/Myc-VAMP5 cells showed no difference compared with control cells (Figure 1D, right).

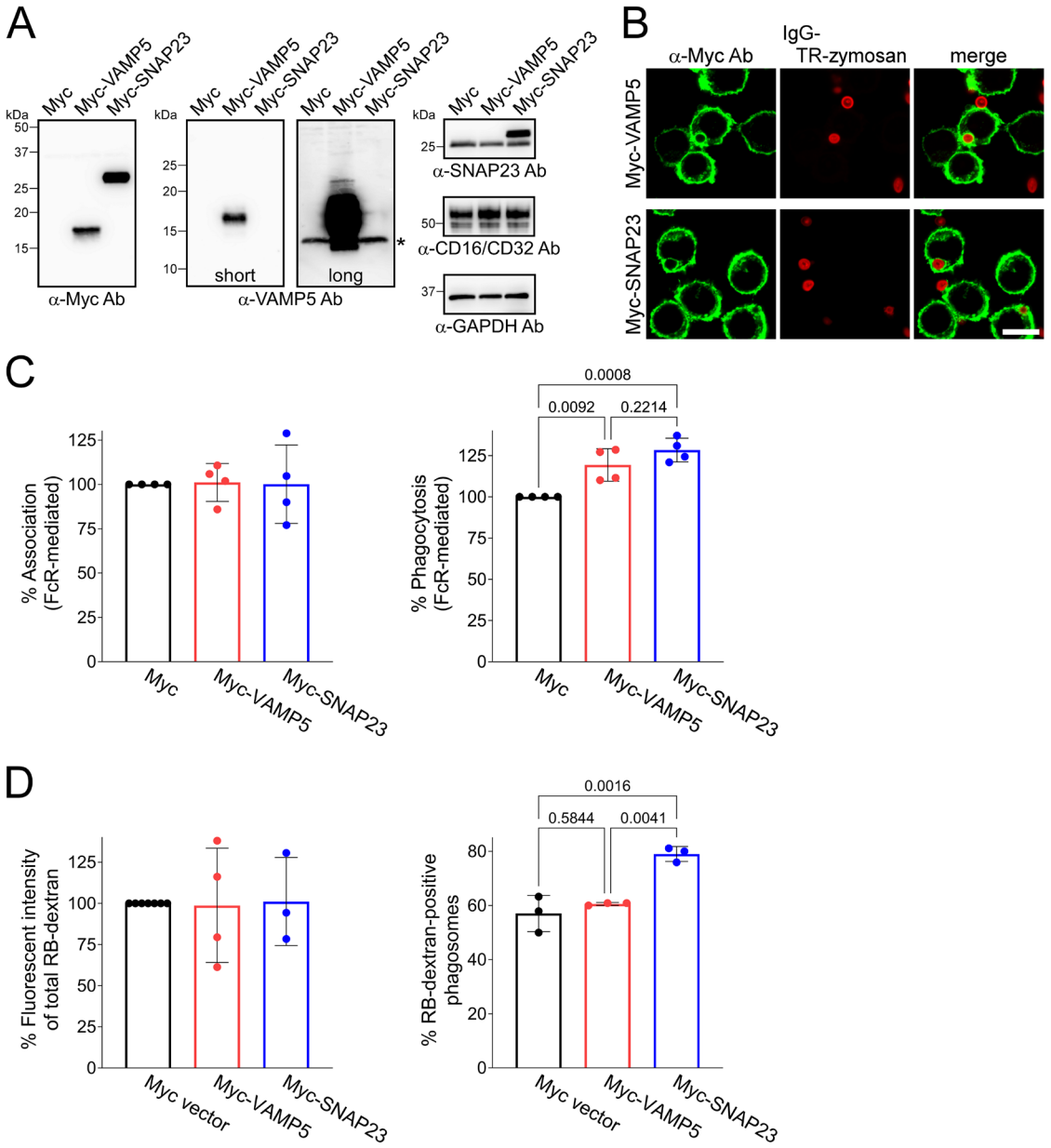

FIGURE 1: Overexpression of Myc-tagged VAMP5 in J774 macrophages enhances FcR-mediated phagocytosis but not phagosome-lysosome fusion. (A) Total lysates from J774 macrophages stably expressing Myc-tag, Myc-VAMP5, and Myc-SNAP23 were analyzed by western blotting using the indicated antibodies. Asterisk denotes endogenous VAMP5. (B) Immunofluorescence imaging of J774/Myc-VAMP5 and J774/Myc-SNAP23 cells after ingesting IgG-opsonized Texas Red-conjugated zymosan A (IgG-TR-zymosan) particles. Scale bar: 10 μm. (C) J774/Myc, J774/Myc-VAMP5, and J774/Myc-SNAP23 cells were incubated with IgG-TR-zymosan, and the efficiencies of association (left) and phagocytosis (right) were then measured. Arbitrary fluorescence units were normalized to the value obtained for J774/Myc cells within the same experiment, defined as 100%. Data are presented as the mean ± standard error of the mean (SEM) of four independent experiments. (D) J774 cells expressing Myc constructs were preloaded with RB-dextran to label late endosomes/lysosomes. Total RB fluorescence was measured to serve as an indicator of labeling efficiency (left). The percentage of RB-dextran-positive phagosomes (more than 30 individual phagosomes from at least 30 different cells were measured in each experiment) was calculated (right). Data are presented as the mean ± SEM of three to four (left) or three (right) independent experiments. Statistical analyses were performed using one-way ANOVA with Tukey's post hoc test (the decimal numbers above the bars represent the *p* values).

Knockdown of *VAMP5* suppresses FcR-mediated phagocytosis but not phagosome-lysosome fusion

To confirm the effect of Myc-VAMP5 overexpression on phagocytosis (as shown in Figure 1), we performed experiments using small interference RNA (siRNA)-mediated knockdown of *VAMP5*. As shown in Figure 2A, similar to the case for the transfection with SNAP23 siRNA, endogenous VAMP5 expression was sufficiently reduced in J774 cells transfected with mouse VAMP5 siRNA compared with that in the cells transfected with control siRNA. We then examined the phagocytosis efficiency of these knockdown cells

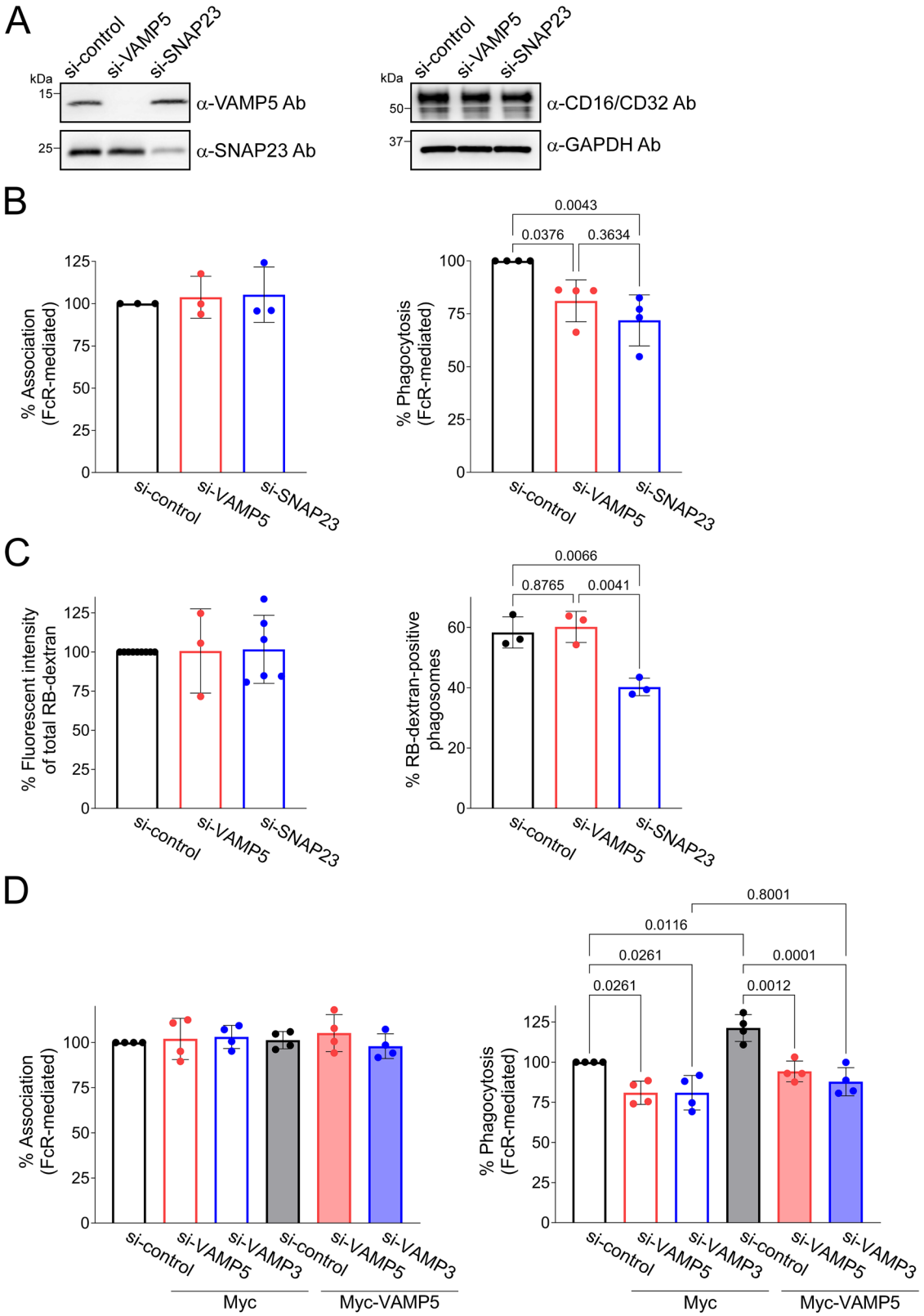

FIGURE 2: Knockdown of *VAMP5* suppresses FcR-mediated phagocytosis but not phagosome-lysosome fusion. (A) Total cell lysates from J774 cells 72 h after transfection with a nonspecific control siRNA (si-control), VAMP5 siRNA (si-VAMP5), and SNAP23 siRNA (si-SNAP23) were analyzed by western blotting with the indicated antibodies. (B) siRNA-transfected cells were incubated with IgG-opsonized Texas Red-zymosan, and the efficiencies of association (left) and phagocytosis (right) were measured, as described in Figure 1C. Data are presented as the mean ± SEM of three (left) or four (right) independent experiments. (C) siRNA-transfected cells labeled late endosomes/lysosomes with RB-dextran and total RB fluorescence were measured (left). The percentage of RB-dextran-positive phagosomes was

using IgG-TR-zymosan particles. Herein, we found that the phagocytosis efficiency of *VAMP5*-knockdown cells (si-VAMP5) was significantly reduced compared with that of control cells (si-control; Figure 2B, right). However, there was no difference in association efficiency between the knockdown cells (Figure 2B, left). Furthermore, we explored the effect of *VAMP5* knockdown on phagosome–lysosome fusion and found that the phagosome–lysosome fusion efficiency was reduced in J774 cells transfected with SNAP23 siRNA but not with VAMP5 siRNA, which was similar to control siRNA (Figure 2C, right). The efficiency of RB-dextran staining of endosomes/lysosomes in siRNA-transfected cells was comparable (Figure 2C, left). To further validate the specificity of VAMP5 siRNA, J774/Myc, and J774/Myc-VAMP5 cells were transfected with VAMP5 siRNA. After confirming the intensive knockdown of Myc-VAMP5 by VAMP5 siRNA (Supplemental Figure S1), these cells were examined by performing the same phagocytosis experiment as in Figure 2B. As a positive control, we examined siRNA against *VAMP3*, which has been shown to function in phagocytosis (Bajno *et al.*, 2000; Braun *et al.*, 2004). In J774/Myc cells, both siRNAs elicited a similar significant reduction in phagocytosis efficiency compared with si-control (Figure 2D, right). The enhanced phagocytosis efficiency observed in J774/Myc-VAMP5 cells (Figure 1C, right) was significantly reduced in VAMP5 siRNA-transfected cells compared with those transfected with control siRNA (Figure 2D, right), indicating that VAMP5 siRNA specifically targets *VAMP5*. Transfection of VAMP3 siRNA also reduced the phagocytosis efficiency in J774/Myc-VAMP5 cells, suggesting the absence of functional redundancy between VAMP5 and VAMP3.

Myc-VAMP5 interacts not only with SNAP23 but also with several Q-SNARE proteins in macrophages

As an R-SNARE protein, VAMP5 could form a SNARE complex with Qa- and Qbc-SNARE proteins during phagocytosis. Based on our previous data, SNAP23 is a candidate Qbc-SNARE protein that forms a complex with VAMP5. Therefore, to characterize the interaction between VAMP5 and other Q-SNARE proteins, immunoprecipitation experiments were performed using lysates from J774 cells expressing Myc-VAMP5 (Figure 3; Supplemental Figure S2). Similar to the previous results, the coprecipitation of Myc-VAMP5 with SNAP23 was confirmed; however, coprecipitation with SNAP29, another Qbc-SNARE protein, was not detected. For all other Q-SNAREs that could be examined, Myc-VAMP5 interacted with the plasmalemma Qa-SNAREs syntaxin 3 (stx3) and stx4 but not with stx2 and stx11. Notably, Myc-VAMP5 also coprecipitated with other Qa-SNAREs, stx5 short isoform (35 kDa, Golgi-localized), stx7 (endosomal), stx13 (recycling endosomal), stx18 (ER-localized), and Qb-SNARE Vti1B (endosomal; Dingjan *et al.*, 2018). These interactions suggest that a small portion of Myc-VAMP5 localized in endomembrane compartments (Figure 1B) could be involved in membrane trafficking between these organelles in macrophages. Given the similar effects of Myc-VAMP5 and Myc-SNAP23 on phagocytosis (Figure 1C) and the interaction between Myc-VAMP5 and SNAP23 previously observed using a single-molecule FRET-based SNAP23 probe (Sakurai *et al.*, 2012), both SNARE proteins may form a noncanonical acceptor complex (consisting of R-SNARE and Qbc-SNARE) on the plasma membrane for fusion with vesicles containing Qa-SNARE derived from the endomembrane compartments during phagocytosis. This may corroborate the findings of a previous report, revealing that, unlike other VAMP proteins, VAMP5 is unable to mediate fusion with acceptor complexes comprising stx1/SNAP25 or stx4/SNAP25 (Hasan *et al.*, 2010).

Phagosome-localized Myc-VAMP5 dissociates before phagosome maturation proceeds

Herein, we detected no involvement of VAMP5 in the progression of phagosome maturation, regardless of its localization to the phagosomal membrane. Thus, to verify the relationship between phagosomal Myc-VAMP5 and phagosome maturation, we used latex beads conjugated with TagGFP2 (p*K*a = 5.0), a pH-sensitive fluorescent protein (Chudakov *et al.*, 2010), to monitor the phagosomal acidification status. We first examined the fluorescence sensitivity of TagGFP2-bound beads to acidic environments under in vitro conditions (Supplemental Figure S3). The fluorescence intensity of TagGFP2-bound beads decreased in 100% methanol (Met-OH), the cell fixation condition. A similar decrease in fluorescence intensity was observed after treatment with citrate buffer (pH 4.4) and then replacing it with phosphate-buffered saline (PBS; pH 7.4); additionally, the fluorescence intensity was markedly reduced upon further treatment with 100% methanol. Neutralizing the acidic environment with PBS did not recover the fluorescent signal; the TagGFP2 protein remained mostly bound to the beads, as judged by staining with an anti-EGFP (enhanced green fluorescent protein) antibody and its secondary antibody (Alexa 555; Supplemental Figure S3). These findings suggest that the fluorescent signal of TagGFP2-bound beads is sensitive to acidic environments without the detachment of TagGFP2 from the beads. Given that the utility of TagGFP2-bound beads was confirmed, J774 cells expressing Myc-VAMP5 or Myc-SNAP23 were loaded with IgG-opsonized TagGFP2-bound beads and then incubated for 1 h for phagosome formation. Subsequently, the cells were fixed and stained with an anti-Myc antibody to visualize Myc-proteins localized in cells (Figure 4A). To distinguish from engulfed beads, beads outside the cell were stained with antirabbit IgG-Alexa Fluor 647 before fixation. Under the microscope, phagosomes containing TagGFP2-bright or -dim beads were classified as positive and negative for Myc-signal, respectively (Figure 4, B and C). Considering phagosomes containing TagGFP2-bright or -dim beads, the former represents nascent or early phagosomes, while the latter represents acidic late phagosomes or phagolysosomes. More than 80% of phagosomes containing TagGFP2-bright beads were positive for Myc-VAMP5 and Myc-SNAP23. Of the phagosomes containing TagGFP2-dim beads, Myc-SNAP23-positive phagosomes accounted for more than 80%, while the proportion of Myc-VAMP5-positive phagosomes was less than 20% (Figure 4C). Accordingly, these results suggest that Myc-VAMP5 dissociates from early phagosome before acidification, and therefore, does not directly impact phagosome maturation.

calculated, as described in Figure 1D (right). Data are presented as the mean ± SEM of three to six (left) or three (right) independent experiments. (D) J774/Myc and J774/Myc-VAMP5 cells transfected with the indicated siRNAs were analyzed for association and phagocytosis efficiencies. The efficiencies of association (left) and phagocytosis (right) in siRNA-transfected cells were measured, as described in Figure 1C. Statistical analyses were performed using one-way ANOVA with Tukey's post hoc test (the decimal numbers above the bars represent the *p* values).

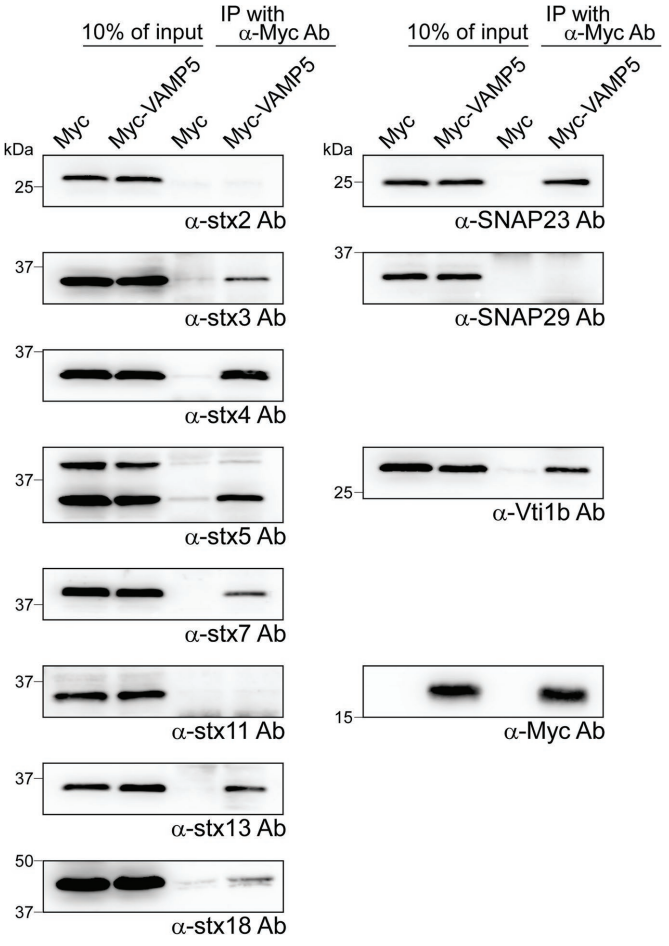

FIGURE 3: Myc-VAMP5 interacts with SNAP23 and several Q-SNARE proteins. J774 cells stably expressing Myc-tag or Myc-VAMP5 were lysed, and the lysates were immunoprecipitated (IP) with an anti-Myc antibody. The immunocomplexes were subjected to SDS–PAGE and Western blot analysis using indicated antibodies. Stx2, stx3, stx4, stx5, stx7, stx11, stx13, and stx18 are Qa-SNARE proteins, SNAP23 and SNAP29 are Qbc-SNARE proteins, and Vti1B is a Qb-SNARE protein.

Dissociation of Myc-VAMP5 from phagosomes depends on the activity of both clathrin and dynamin during phagosome maturation

The nascent phagosome progressively undergoes multiple fusion and fission events with vesicles of the endocytic pathway. Therefore, the decrease in the number of Myc-VAMP5-positive phagosomes observed in Figure 4 could be associated with a fission event on the phagosome. We first examined the effect of dynasore (Macia *et al.*, 2006), which prevents the GTPase activity of dynamin, on the dissociation of Myc-VAMP5 from phagosomes. In vehicle-incubated control cells, we found that the number of Myc-VAMP5-positive phagosomes reduced by more than 60% within 30 min. Conversely, in cells incubated in the presence of dynasore, the decrease in the number of Myc-VAMP5-positive phagosomes was significantly suppressed, probably due to delayed dissociation of Myc-VAMP5 (Figure 5A). Another dynamin inhibitor that blocks the recruitment of dynamin to membranes, MiTMAB (myristyl trimethyl ammonium bromide; Quan *et al.*, 2007; Preta *et al.*, 2015), also suppressed the decrease in the number of Myc-VAMP5-positive phagosomes (Figure 5B), indicating the involvement of dynamin in the dissociation of Myc-VAMP5 from phagosomes.

During apoptotic cell clearance in *Caenorhabditis elegans*, phagosome maturation is regulated by dynamin, clathrin, and adaptor protein 2 (AP2; Kinchen *et al.*, 2008; Chen *et al.*, 2013). The recruitment of clathrin on phagosomes has been observed in mammalian cells and is known to play a crucial role in phagosome maturation and resolution (Tse *et al.*, 2003; Lancaster *et al.*, 2021). Thus, to elucidate the role of clathrin in Myc-VAMP5 dissociation, we employed Pitstop 2, a small molecule compound that inhibits the function of clathrin by binding to the terminal domain (von Kleist *et al.*, 2011). As shown in Figure 5C, treatment with Pitstop 2 markedly suppressed the decrease in the number of Myc-VAMP5-positive phagosomes, indicating that clathrin activity is required for the dissociation of Myc-VAMP5 from phagosomes. These results suggest that both clathrin and dynamin are needed for the dissociation of VAMP5 from early phagosomes during FcR-mediated phagocytosis. However, whether VAMP5 is a direct cargo for clathrin and adaptor proteins or codissociates with specific cargoes of clathrin and adaptor proteins by default remains unclear.

The amino acid sequence of mouse VAMP5 revealed a "YLGL" sequence localized at residues 72–75 near the transmembrane domain of VAMP5 (Supplemental Figure S5C). This sequence matches the YxxΦ motif (in which x is any residue and Φ is a bulky, hydrophobic residue) that is recognized by and interacts with clathrin adaptor proteins (Ohno *et al.*, 1995). Thus, we investigated the potential effect of the "YLGL" sequence on the dissociation of Myc-VAMP5 from early phagosomes. We constructed two mutants, one in which the Tyr72 residue was altered to an alanine residue and the other in which all four amino acid residues were replaced with alanine residues (designated as Y72A and AAAA, respectively; Supplemental Figure S5C). In stably transformed J774 cells, each mutant was localized at the plasma membrane and was expressed at almost the same level as Myc-VAMP5 wild type (WT; Supplemental Figures S4A and S5A). J774 cells expressing each Myc-VAMP5 mutant were examined by performing dissociation analysis using IgG-opsonized beads. The decrease in the number of Myc-VAMP5-positive phagosomes observed in control Myc-VAMP5 WT cells was significantly delayed and suppressed in Myc-VAMP5 AAAA cells (Figure 5D; Supplemental Figure S6) but not in Myc-VAMP5 Y72A cells (Supplemental Figure S5B, left). These results suggest that the "YLGL" sequence of VAMP5 is important for dissociation from phagosomes, but does not function as a "YxxΦ" motif. Hence, whether Myc-VAMP5 WT interacts with clathrin or dynamin in the presence of dynamin inhibitors is uncertain.

We next determined whether clathrin and dynamin are localized to the phagosomal membrane in the presence of dynamin inhibitors in J774 cells expressing Myc-VAMP5 WT and Myc-VAMP5 AAAA. Upon transiently expressing both mVenus-clathrin light chain (mV-CLC) and mScarlet-dynamin 2 (mSc-Dyn2) in J774/Myc-VAMP5 WT cells, we detected an increase in the number of mV-CLC-positive and mSc-Dyn2-positive phagosomes in the presence of dynasore and MiTMAB (Figure 5, E and F). However, in the presence of MiTMAB, the number of mSc-Dyn2-positive phagosomes was reduced compared with that in the presence of dynasore. This finding could be attributed to the inhibitory effect of MiTMAB on the binding of dynamin to the membrane. In contrast, there was no significant increase in the number of mV-CLC-positive and mSc-Dyn2-positive phagosomes in J774/Myc-VAMP5 AAAA cells, even in the presence of dynamin inhibitors (Figure 5, E and F).

Taken together, these results suggest that at least the "YLGL" sequence of VAMP5 is crucial for clathrin- and dynamin-dependent dissociation from early phagosomes and interaction with clathrin and dynamin, although it remains unclear whether it binds directly to the AP complex.

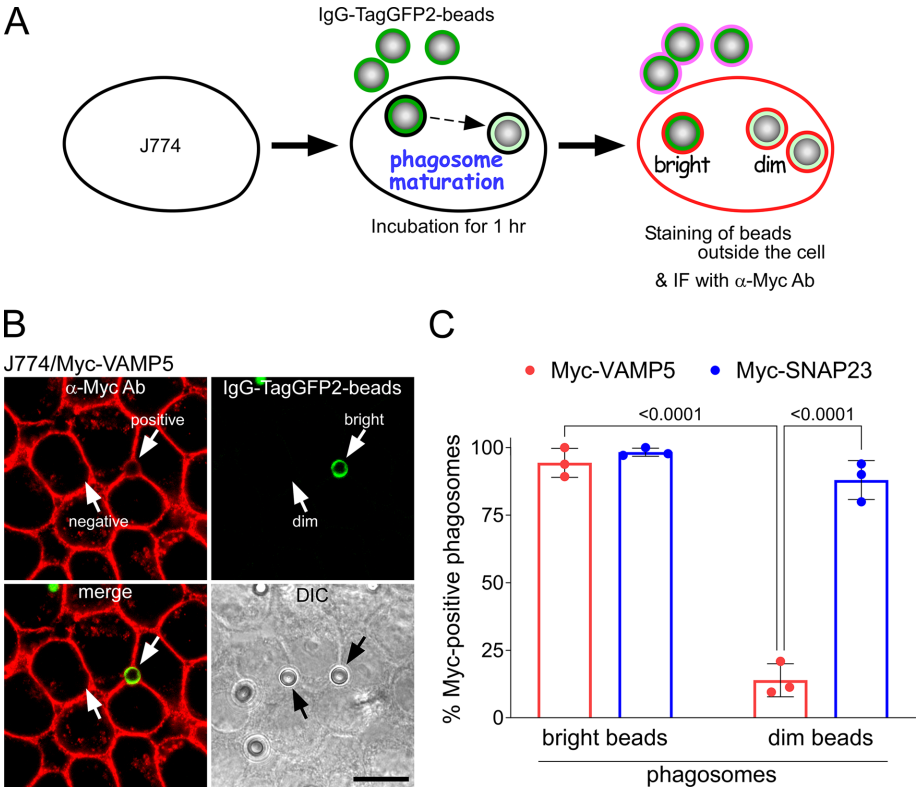

FIGURE 4: Phagosome-localized Myc-VAMP5 dissociates before the progression of phagosome maturation. (A) J774/Myc-VAMP5 and J774/Myc-SNAP23 cells were incubated with IgG-opsonized TagGFP2-bound beads at 37°C for 1 h. After staining the beads outside the cells with Alexa Fluor 647-donkey antirabbit secondary antibodies to distinguish them from engulfed beads, the cells were fixed and immunostained with an anti-Myc antibody, followed by Alexa Fluor 555-goat antimouse secondary antibodies. The fluorescence sensitivity of TagGFP2-bound beads to acidic environments was confirmed under in vitro conditions (Supplemental Figure S3). (B) The arrows indicate phagosomes containing TagGFP2-bound beads with bright or dim fluorescence signals. Nascent/early phagosomes contain beads with a bright fluorescence signal, while phagosomes containing beads with a dim fluorescence signal indicate the formation of an acidic milieu with maturation. Scale bar: 10 μm. (C) Phagosomes containing the above two types of beads were further classified as Myc-positive (Alexa Fluor 555-positive) or -negative phagosomes. In each experiment, more than 150 phagosomes containing beads were classified, and the percentage of Myc-positive phagosomes per bright and dim beads was calculated. Data are presented as mean ± SEM of three independent experiments. Statistical analysis was performed using two-way ANOVA with Tukey's post hoc test (the decimal numbers above the bars represent the *p* values).

Dissociation of Myc-VAMP5 from early phagosomes shifts SNAP23 into an acceptable structure for subsequent membrane fusion, leading to phagosome maturation

Dissociation of VAMP5 from early phagosomes implies the termination of its function in phagosome formation and may be necessary for phagosome maturation in the subsequent step. To investigate this possibility, after the same procedure as in Figure 5, we performed immunofluorescence experiments to visualize the phagosome localization of lysosomal-associated membrane protein 1 (LAMP1). In J774/Myc-VAMP5 WT cells, the number of LAMP1-positive phagosomes owing to phagosome maturation increased gradually by more than 70% within 30 min. In contrast, this increase was noticeably suppressed in cells incubated in the presence of Pitstop 2 (Figure 6A, left). To clarify whether this Pitstop 2-mediated reduction in the number of LAMP1-positive phagosomes (Figure 6A, left) was due to Myc-VAMP5 overexpression, we next examined J774/Myc cells in the same experiment. In the presence of Pitstop 2, the time course profile of the number of LAMP1-positive phagosomes was only reduced to ~40–50% compared with the 20% observed in J774/Myc-VAMP5 cells (Figure 6A, right). A similar reduction was observed in J774/Myc-VAMP5 AAAA cells without Pitstop 2 (Figure 6B). These results indicate that Myc-VAMP5, accidentally retained on the phagosome, may interfere with subsequent phagosome maturation by SNAP23 during FcR-mediated phagocytosis (Sakurai *et al.*, 2012).

We previously developed a SNAP23 intramolecular FRET probe (named tG-S1-tR-S2), incorporated with the fluorescent proteins TagGFP2 and TagRFP at the N-terminus of two SNARE motifs, to clarify its structural alteration at the phagosomal membranes (Sakurai *et al.*, 2012, 2018). The FRET signal was enhanced when the probe adopted a closed conformation upon SNARE complex formation. Subsequently, we examined the availability of this FRET probe in the cells used in the current study. Consistent with our previous results (Sakurai *et al.*, 2012), transient expression of tG-S1-tR-S2 significantly enhanced the FRET signal at the plasma membrane in J774/Myc-VAMP5 WT cells compared with J774/Myc cells. Similarly, a significant increase in the FRET signal of tG-S1-tR-S2 was observed in J774/Myc-VAMP5 AAAA cells (Supplemental Figure S4C). Next, to examine the effect of Pitstop 2 on SNAP23 dynamics at the phagosomal membranes, J774/Myc or J774/Myc-VAMP5 cells were transiently expressed with the tG-S1-tR-S2 probe. Control J774/Myc cells displayed a slight enhancement in the FRET signal from tG-S1-tR-S2 on phagosomes containing IgG-opsonized zymosan in the presence of Pitstop 2; however, the difference was not significant compared with the vehicle-treated cells according to multiple comparison testing (Figure 6C). In contrast, treatment with Pitstop 2 significantly enhanced the FRET signal in J774/Myc-VAMP5 cells (Figure 6C). Notably, in J774/Myc-VAMP5 AAAA cells expressing the tG-S1-tR-S2 probe, enhanced FRET signals were detected on phagosomes despite the absence of Pitstop 2 (Figure 6D). These results suggest that Myc-VAMP5 retained on phagosomes may continuously interact with SNAP23 to maintain a closed conformation, thereby interrupting SNAP23-mediated membrane fusion for subsequent phagosome maturation. In the phagosome–lysosome fusion assay, J774/Myc-VAMP5 AAAA cells showed significantly decreased numbers of RB-dextran-positive phagosomes compared with J774/Myc-VAMP5 WT cells (Supplemental Figure S4E, right).

DISCUSSION

SNAP23 regulates FcR-mediated phagocytosis in macrophages, but the appropriate SNARE partners of SNAP23 involved in phagosome formation remain unclear. We have previously reported that VAMP5 is a SNARE protein that interacts with SNAP23 and forces it into a

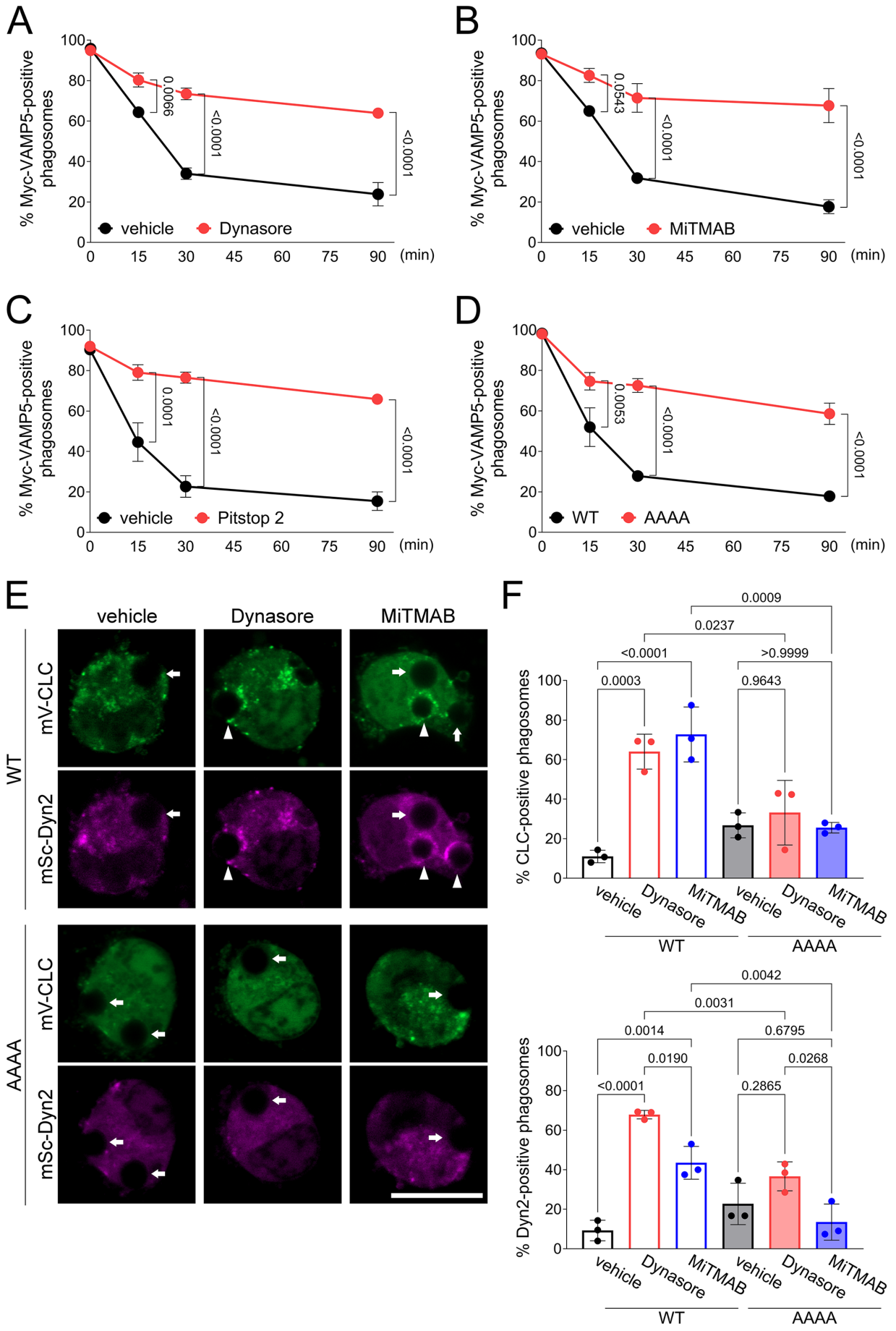
A
% Myc-VAMP5-positive phagosomes
vehicle
Dynasore
0.9966
<0.0001
<0.0001
(min)
B
% Myc-VAMP5-positive phagosomes
vehicle
MiTMAB
0.0543
<0.0001
<0.0001
(min)
C
% Myc-VAMP5-positive phagosomes
vehicle
Pitstop 2
0.1001
<0.0001
<0.0001
(min)
D
% Myc-VAMP5-positive phagosomes
WT
AAAA
0.0053
<0.0001
<0.0001
(min)
E
vehicle
Dynasore
MiTMAB
WT
mV-CLC
mSc-Dyn2
AAAA
mV-CLC
mSc-Dyn2
F
% CLC-positive phagosomes
0.0009
0.0237
<0.0001
>0.9999
0.0003
0.9643
vehicle
Dynasore
MiTMAB
vehicle
Dynasore
MiTMAB
WT
AAAA
% Dyn2-positive phagosomes
0.0042
0.0031
0.0014
0.6795
0.0190
0.0268
<0.0001
0.2865
vehicle
Dynasore
MiTMAB
vehicle
Dynasore
MiTMAB
WT
AAAA

closed conformation at the macrophage plasma membrane (Sakurai *et al.*, 2012). However, the precise step at which VAMP5 participates in intracellular membrane trafficking and whether VAMP5 functions in phagocytosis are yet to be established. To the best of our knowledge, this is the first study to demonstrate that VAMP5 positively regulates phagosome formation but does not directly regulate phagosome maturation in FcR-mediated phagocytosis. Moreover, we present evidence that the rapid dissociation of VAMP5 from the phagosomal membrane depends on clathrin and dynamin activity and is essential for promoting the formation of open SNAP23 required for SNARE-mediated membrane fusion during phagosome maturation (Figure 6E).

VAMP5 regulates FcR-mediated phagocytosis in macrophages

J774 macrophages transfected with VAMP5 siRNA downregulated the phagocytosis of IgG-opsonized zymosan (Figure 2B, right), which was enhanced by J774 cells stably overexpressing Myc-VAMP5 (Figure 1C, right). This enhancement was canceled by introducing VAMP5 siRNA (Figure 2D, right), demonstrating that VAMP5 positively regulates FcR-mediated phagocytosis in macrophages. Given that the expression of endogenous VAMP5 is relatively lower than that of SNAP23, as roughly indicated by the western blot data (Figure 1A), the effect of VAMP5 siRNA-mediated knockdown on phagocytosis was expected to be robust but was found to be relatively weak (Figure 2B, right). This may indicate that VAMP5 partially functions in FcR-mediated phagocytosis in parallel with other VAMP protein(s). This possibility is strongly supported by previous reports, demonstrating that VAMP3 and VAMP7 participate in FcR-mediated phagocytosis (Bajno *et al.*, 2000; Braun *et al.*, 2004). The effect of VAMP3 siRNA-mediated knockdown was comparable with that of VAMP5 siRNA in J774/Myc cells, at least when using our phagocytosis analysis system (Figure 2D, right). These VAMP proteins required for FcR-mediated phagosome formation may be selected according to the specific situation, such as the positional relationship between the intracellular organelles and the plasma membrane. Given that VAMP3 also participates in the phagocytosis of *Candida albicans* in macrophages (Murray *et al.*, 2005), VAMP5 may also be required for other types of phagocytosis. Focusing on membrane fusion, during FcR-mediated phagocytosis, VAMP5 is expected to cooperate with SNAP23 at the plasma membrane to mediate SNARE complex formation with unidentified syntaxin (Qa-SNARE) localized in organelle-derived vesicles (Sakurai *et al.*, 2012). According to the results of immunoprecipitation experiments, VAMP5 could interact with candidate syntaxins, such as stx5 (Golgi-localized), stx7 (late endosome/lysosome-localized), stx13 (recycling endosome-localized), and stx18 (ER-localized; Figure 3). Further investigation is needed to identify the SNARE proteins that can partner with VAMP5, responsible for FcR-mediated phagocytosis.

VAMP5 rapidly disappears from early maturing phagosomes

Myc-VAMP5 disappeared from early maturing phagosomes containing IgG-opsonized particles in J774/Myc-VAMP5 cells. The disappearance of Myc-VAMP5 from the phagosome could be due to pinching off by tubulation/scission or vesiculation and (or) internalization within the phagosome by inward budding via intraluminal vesicle for degradation (Fairn and Grinstein, 2012; Lancaster *et al.*, 2021; Levin-Konigsberg and Mantegazza, 2021). Our microscopic analysis failed to detect any Myc-VAMP5 signal within phagosomes where the surface Myc-VAMP5 signal had already disappeared (Figure 4B; Supplemental Figure S6). Thus far, outward tubulation/vesiculation from the phagosome triggers Myc-VAMP5 dissociation. During the early stages of phagosome maturation, several proteins, such as sorting nexin family proteins, clathrin, the clathrin adaptor protein complex AP2, and dynamin, were found to participate in fission and (or) tubulation from the phagosome and promote maturation (Kinchen *et al.*, 2008; Gopaldass *et al.*, 2012; Chen *et al.*, 2013). Previous studies in *C. elegans* have suggested that dynamin activity might be required for the small GTPase Rab5 recruitment to phagosomes, forming a complex with clathrin, AP2, and the sorting nexin 9-family protein LST-4 to progress phagosome maturation during phagocytosis of apoptotic cells (Chen *et al.*, 2013). Consistent with these reports, treatment with inhibitors of clathrin and dynamin could suppress Myc-VAMP5 dissociation from early phagosomes (Figure 5). Nevertheless, the mechanism through which clathrin and dynamin dissociate VAMP5 from phagosomes remains elusive.

In certain animal species, such as rodents and cattle, VAMP5 has been shown to possess an AP2-recognized YxxΦ motif (72-YLGL-75) on the cytoplasmic side, in close proximity to its transmembrane domain (Ohno *et al.*, 1995). Indeed, J774 cells expressing the Myc-VAMP5 AAAA mutant were found to be defective in terms of dissociation from phagosomes (Figure 5D), whereas Myc-VAMP5 Y72A, another mutant with only one amino acid substitution, dissociated from phagosomes in almost the same manner as the WT (Supplemental Figure S5B). In addition, in animal species such as humans, chimpanzees, and horses, VAMP5 possesses 72C instead

FIGURE 5: Dissociation of Myc-VAMP5 from phagosomes depends on the activity of both clathrin and dynamin during phagosome maturation. (A, B, and C) J774/Myc-VAMP5 WT cells were incubated with IgG-opsonized beads in the presence of dimethyl sulfoxide (DMSO; vehicle), dynasore, MiTMAB, or Pitstop 2 at 30°C and subjected to immunofluorescence staining with an anti-Myc antibody at the indicated time point. (D) J774/Myc-VAMP5 WT and J774/Myc-VAMP5 AAAA cells were incubated for 5 min at 30°C and subjected to immunofluorescence staining with an anti-Myc antibody at the indicated time point. In each experiment, more than 30 individual phagosomes were measured from at least 30 different cells, and the percentage of Myc-positive phagosomes relative to the total number of phagosomes was calculated. (E) J774/Myc-VAMP5 WT and J774/Myc-VAMP5 AAAA (AAAA) cells were transiently cotransfected with plasmids of mV-CLC and mSc-Dyn2. Sixteen hours after transfection, cells were incubated with IgG-opsonized latex beads for 5 min at 30°C to initiate phagocytosis. The cells were then washed and incubated in HBSS containing DMSO, dynasore, or MiTMAB for 30 min at 30°C in the presence of cytochalasin B to inhibit the formation of new phagosomes. The triangles and arrows indicate mV-CLC or mSc-Dyn2-positive and -negative phagosomes, respectively. Scale bar: 10 μm. (F) The number of phagosomes of each type shown in (E) was quantified. In each experiment, more than 30 phagosomes were counted and classified as phagosomes with (positive) and without (negative) obvious signals. Data are presented as mean ± SEM of three (A, B, and F) or four (C and D) independent experiments. Statistical analyses were performed using two-way ANOVA with Tukey's post hoc test (the decimal numbers above the bars represent the *p* values).

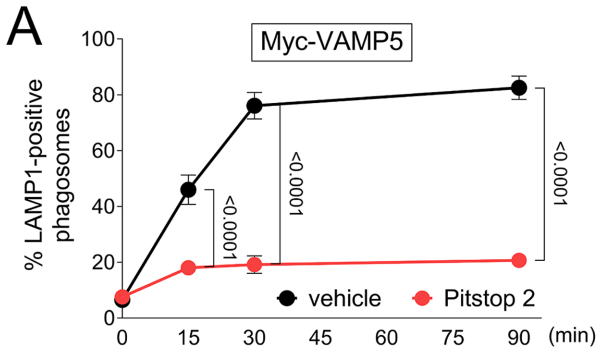
A
Myc-VAMP5
% LAMP1-positive phagosomes
100
80
60
40
20
0
0
15
30
45
60
75
90
(min)
<0.0001
<0.0001
<0.0001
vehicle
Pitstop 2

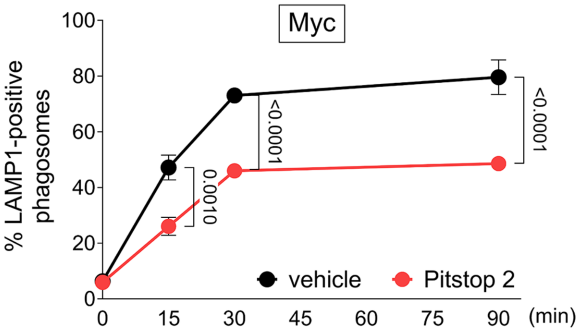
Myc
% LAMP1-positive phagosomes
100
80
60
40
20
0
0
15
30
45
60
75
90
(min)
<0.0001
<0.0001
0.0010
vehicle
Pitstop 2

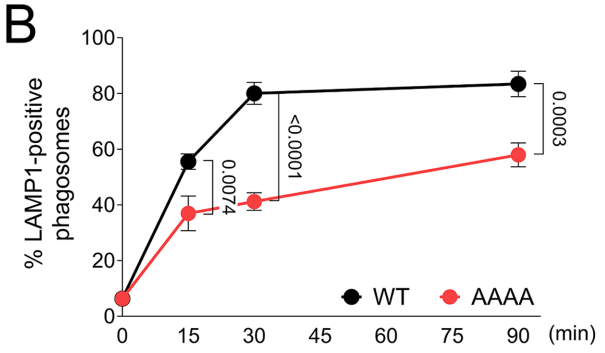
B
% LAMP1-positive phagosomes
100
80
60
40
20
0
0
15
30
45
60
75
90
(min)
<0.0001
0.0074
0.0003
WT
AAAA

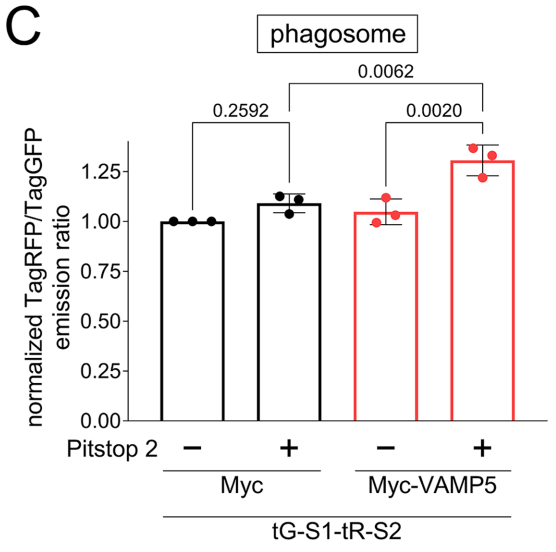
C
phagosome
0.0062
0.2592
0.0020
normalized TagRFP/TagGFP emission ratio
1.25
1.00
0.75
0.50
0.25
0.00
Pitstop 2
–
+
–
+
Myc
Myc-VAMP5
tG-S1-tR-S2

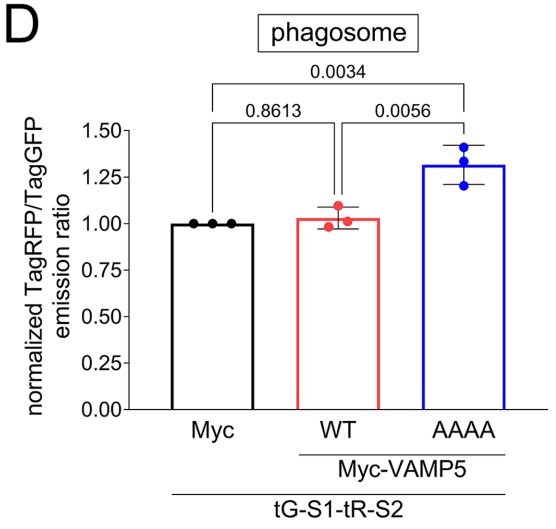
D
phagosome
0.0034
0.8613
0.0056
normalized TagRFP/TagGFP emission ratio
1.50
1.25
1.00
0.75
0.50
0.25
0.00
Myc
WT
AAAA
Myc-VAMP5
tG-S1-tR-S2

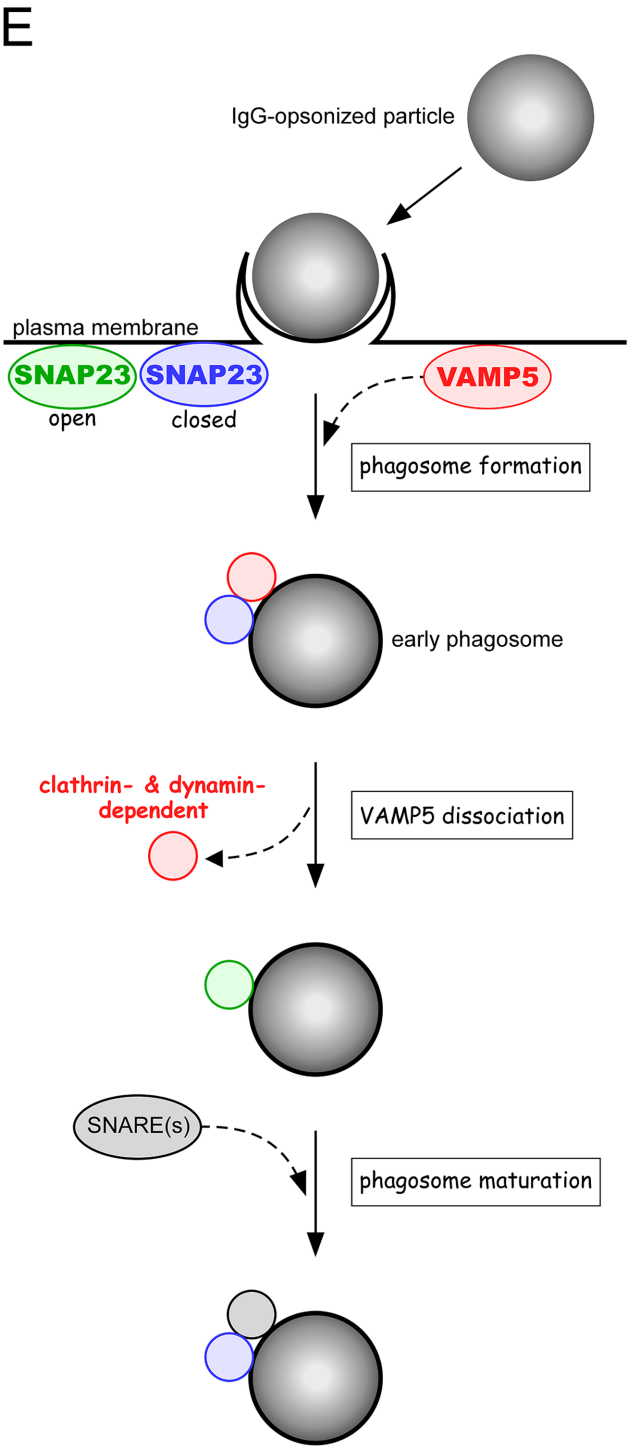
E
IgG-opsonized particle
plasma membrane
SNAP23
open
SNAP23
closed
VAMP5
phagosome formation
early phagosome
clathrin- & dynamin-dependent
VAMP5 dissociation
SNARE(s)
phagosome maturation

of 72Y, which does not match the typical YxxΦ motif (Supplemental Figure S5C). These findings suggest that the "YLGL" sequence is unlikely to be the AP2-recognition motif, and the AAAA mutant may affect the interaction between the lipid bilayer and the transmembrane domain of VAMP5. However, regarding the expression level and localization of the Myc-VAMP5 AAAA mutant (Supplemental Figure S4A), interaction with SNAP23 and phagocytosis efficiency (Supplemental Figure S4, B–D) are markedly similar to those of Myc-VAMP5 WT in J774 cells. Our results demonstrate that the "YLGL" sequence is at least required for clathrin- and dynamin-dependent dissociation of VAMP5 from the early phagosome. Further characterization of this sequence should be undertaken in future investigation, as it may be a direct target of AP2 or may be necessary for binding to target cargo proteins of AP2 and clathrin that dissociate from early phagosomes.

Dissociation of VAMP5 allows the activation of SNAP23, which subsequently participates in phagosome maturation

Dissociation of VAMP5 from early phagosomes is speculated to have at least two physiological implications: one is the recycling of VAMP5 to the plasma membrane for the subsequent round of phagosome formation; the other is a checkpoint function to progress subsequent proper phagosome maturation. Maintenance of phagosomal size and sequential maturation may require several checkpoints to sense the environment and contents of the phagosome and phagosomal membrane precisely; however, these mechanisms remain poorly understood. SNAP23 on the phagosomal membrane is thought to take an open conformation required for subsequent SNARE complex formation during phagosome maturation. Using an intramolecular FRET probe of SNAP23, we demonstrated that the FRET signal from this probe was enhanced on the phagosomal membrane in the presence of Pitstop 2 in J774/Myc-VAMP5 cells compared with that in J774/Myc cells (Figure 6C), indicating that Myc-VAMP5 accumulated on phagosomes interacts with SNAP23 to maintain its closed conformation. The results support the more severe reduction in the number of LAMP1-positive phagosomes in J774/Myc-VAMP5 cells in the presence of Pitstop 2 than in J774/Myc cells (Figure 6A). Compared with Myc-VAMP5, the abundance of endogenous VAMP5 is probably lower; this complicates the direct analysis of its function. Indeed, as shown in Supplemental Figure S7, the efficiency of the formation of RB-dextran-positive phagosomes (i.e., phagosome-lysosome fusion efficiency) was comparable between si-control and si-VAMP5-transfected J774 cells in the absence of Pitstop 2, similar to the result shown in Figure 2C, right panel. However, in the presence of Pitstop 2, we observed that this efficiency was clearly decreased to ~ 20 and 40% in si-control and si-VAMP5 cells, respectively. Compared with si-VAMP5 cells, this significant decrease in si-control cells could be due to the failure of endogenous VAMP5 to dissociate from phagosomes. These results suggest that VAMP5 dissociation from the early phagosomes is required for the reuse of SNAP23 in subsequent membrane fusion events, which could be a potential checkpoint to the next step of phagosome maturation.

Assembly of the SNARE complex composed of VAMP5 and SNAP23 may occur beneath the attachment site of IgG-opsonized particles to the plasma membrane. After phagosome formation, disassembly of this complex (*cis*-SNARE complex) on the phagosomal membrane is achieved through the chaperone-like ATPase activity of NSF and α-SNAP (Weber *et al.*, 2000). The enhanced FRET signal of the SNAP23 probe on the phagosomal membrane was detected in J774/Myc-VAMP5 WT cells in the presence of a clathrin inhibitor (Figure 6C), as well as in J774/Myc-VAMP5 AAAA cells in the absence of the inhibitor (Figure 6D). These results indicate that both Myc-VAMP5 WT and Myc-VAMP5 AAAA in their respective states still form the SNARE complex with SNAP23 and that the NSF/α-SNAP-mediated disassembly of the *cis*-SNARE complex, which comprises Myc-VAMP5 and SNAP23, requires the recruitment and activity of AP2/clathrin to the phagosomal membrane. The defective disassembly of this SNARE complex may be due to the inactivity or lack of localization ability of NSF and α-SNAP. Previously, NSF was found to be localized to clathrin-coated vesicles purified from the human placenta and porcine brain. Furthermore, the NSF-binding site was found to closely overlap the AP2-associated membrane region in the rat synapse (Steel *et al.*, 1996; Lee *et al.*, 2002). These findings suggest that the NSF/α-SNAP function at the disassembly

FIGURE 6: Dissociation of Myc-VAMP5 from early phagosomes shifts SNAP23 into an acceptable structure for subsequent membrane fusion, leading to phagosome maturation. (A) J774/Myc-VAMP5 WT (left) and J774/Myc cells (right) were incubated with IgG-opsonized beads in the presence of DMSO (vehicle) or Pitstop 2 and subjected to immunofluorescence staining with anti-LAMP1 antibodies at the indicated time point. (B) J774/Myc-VAMP5 WT and J774/Myc-VAMP5 AAAA cells were incubated with IgG-opsonized beads and subjected to immunofluorescence staining with anti-LAMP1 antibodies at the indicated time point. In each experiment (A and B), more than 30 individual phagosomes from at least 30 different cells were measured, and the percentage of LAMP1-positive phagosomes per total phagosomes was calculated. Data are presented as mean ± SEM of four independent experiments. Statistical analyses were performed using two-way ANOVA with Tukey's post hoc test (the decimal numbers above the bars represent the *p* values). (C and D) J774/Myc, J774/Myc-VAMP5 WT, and J774/Myc-VAMP5 AAAA cells transiently expressed with SNAP23 FRET probe tG-S1-tR-S2 were incubated with IgG-opsonized zymosan for 30 min on ice and then for 5 min at 37°C. The cells were washed using ice-cold HBSS to remove excess zymosan and incubated for 30 min at 37°C in the presence of cytochalasin B to inhibit the formation of new phagosomes. The fluorescence spectra of tG-S1-tR-S2 on the phagosome membrane were measured, as described in the *Materials and Methods* section. FRET efficiency is represented as the 583/503-nm emission peak ratio (TagRFP/TagGFP2) and normalized to the value obtained from J774/Myc cells in the absence of Pitstop 2, arbitrarily set to 1.00. Data are presented as mean ± SEM of three independent experiments. Statistical analyses were performed using one-way ANOVA with Tukey's post hoc test (the decimal numbers above the bars represent the *p* values). (E) Schematic representation of VAMP5 function in FcR-mediated phagocytosis. VAMP5 participates in FcR-mediated phagocytosis, possibly by cooperating with SNAP23, and then quickly dissociates from early phagosomes. VAMP5 dissociation leaves SNAP23 in an open conformation for subsequent membrane fusion during phagosome maturation. Analysis using specific inhibitors suggests that the activity of clathrin and dynamin mediates this dissociation. Additionally, VAMP5 with a mutated AP-binding motif is less likely to dissociate from the phagosomal membrane. Thus, VAMP5 dissociation is expected to be a checkpoint in the completion of phagosome formation and a critical step in the next stage of phagosome maturation.

site of the SNARE complex may be correlated with AP2/clathrin activity. Therefore, one possible hypothesis is that when the "YLGL" sequence of VAMP5 becomes accessible to AP2 and clathrin or their associated protein(s), NSF and α-SNAP recruited at or near that site may facilitate the disassembly of the *cis*-SNARE complex comprising SNAP23. This leads to VAMP5 dissociation from phagosomes and the formation of open SNAP23, which mediates the progression of subsequent phagosome maturation.

In conclusion, our study provides novel insights into the role of VAMP5 in immunological defense via SNARE-based membrane trafficking during FcR-mediated phagocytosis in macrophages. Importantly, our observation that the dissociation of VAMP5 from early phagosomes regulates the function of SNAP23 in subsequent phagosome maturation contributes to a better understanding of the regulatory mechanisms of this process. As the regulatory processes of phagosome maturation are dependent on both ingested target particles and their specific receptors, future studies are warranted to identify the SNARE proteins corresponding to each receptor and whether they possess regulatory mechanisms similar to VAMP5.

MATERIALS AND METHODS

Request a protocol through *Bio-protocol*.

Antibodies

Polyclonal antibodies against stx5, stx7, stx11, stx18, VAMP3, VAMP5, and EGFP, and monoclonal antibodies against Myc were prepared as described previously (Okumura *et al.*, 2006; Hatsuzawa *et al.*, 2009; Sakurai *et al.*, 2012). The remaining antibodies were obtained from the following commercial sources: stx2 (VAP-SV065) and stx13 (VAM-SV026) from Stressgen (Victoria, Canada); stx3 (N1C2) from Genetex (Irvine, CA); stx4 (S9924), SNAP23 (TS-19), SNAP29 (S2069), Vti1b (HPA044121), and β-actin (A2228) from Sigma-Aldrich (St. Louis, MO); CD16/CD32 (NBP2-52644; FcγIII/FcγII receptors) from Novus Biologicals (Centennial, CO); LAMP1 (1D4B) from Santa Cruz Biotechnology (Santa Cruz, CA); glyceraldehyde-3-phosphate dehydrogenase (AM4300; GAPDH) from Ambion (Austin, TX).

Cell culture

J774 cells were obtained from the Riken Cell Bank (Tsukuba, Japan) and cultured in Roswell Park Memorial Institute (RPMI)-1640 (Fujifilm Wako Pure Chemical Industries, Osaka, Japan) supplemented with 10% fetal bovine serum (FBS) at 37°C in 5% CO_2. J774 cells stably expressing Myc-tagged proteins were maintained in RPMI-1640, supplemented with 10% FBS and 2 μM puromycin to maintain selection. All cell lines were confirmed to be mycoplasma negative every 3 mo using a MycoBlue Mycoplasma Detector (Vazyme, Nanjing, China).

Expression vectors and establishment of stable transformation

Previously, SNAP23 cDNA was obtained by PCR from a MATCHMAKER human leukocyte cDNA library (Clontech, Mountain View, CA), and VAMP5 cDNA was obtained from the total RNA extracted from J774 cells by performing reverse transcription-PCR (Sakurai *et al.*, 2012). cDNAs were cloned into the pcDNA-Myc-C1 vector (Sakurai *et al.*, 2012). The expression vectors pcDNA-Myc-VAMP5 Y72A and pcDNA-Myc-VAMP5 AAAA were created by overlapping PCR and confirmed by DNA sequencing. J774 cell lines stably expressing Myc-tagged proteins were established by infection with recombinant retroviruses generated using cDNAs of Myc-tagged proteins cloned into the pCXpur vector (Akagi *et al.*, 2003).

siRNA experiments

A siRNA duplex with 52% GC content (5′-GUACCGCACGUCAUUCGUAUC-3′; Sigma-Aldrich) served as control. RNA duplexes used for targeting were VAMP5 siRNA (5′-AAUUGUUGAGCAUGAUUUCCG-3′; Sigma-Aldrich) and VAMP3 siRNA (5′-AACCCUUUAAGAAGUUUUUAU-3′; Japan Bio Services, Saitama, Japan) corresponding to the open reading frame of mouse *VAMP5* mRNA and the 3′-untranslated region of mouse *VAMP3* mRNA, respectively. The RNA duplex for mouse *SNAP23* has been described previously (Sakurai *et al.*, 2012). J774 cells or J774 stably expressing Myc-VAMP5 cells were transfected with control (final concentration, 100 nM), VAMP5 (5 nM), SNAP23 (20 nM), or VAMP3 siRNAs (100 nM) using HiPerFect transfection reagent (Qiagen, Hilden, Germany) according to the manufacturer's instructions. The cells were used for subsequent experiments 72 h after transfection.

Western blotting and immunoprecipitation

Cell lysates with extraction buffer (20 mM HEPES-KOH, pH 7.2, 100 mM KCl, 2 mM EDTA, 1 mM Phenylmethylsulfonyl fluoride, 1% TritonX-100, 1 mM dithiothreitol and a protease inhibitor cocktail [Nacalai Tesque, Kyoto, Japan]) were treated with five × sodium dodecyl sulfate-polyacrylamide gel electrophoresis (SDS–PAGE) sample buffer at 95°C. The samples were analyzed by western blotting with various antibodies. The immunoreactive proteins were visualized utilizing ImmunoStar Zeta (Fujifilm Wako Pure Chemical Industries) on the ImageQuant LAS-4000 system (GE Healthcare, Chicago, IL). For immunoprecipitation, lysates from J774 cells stably expressing Myc-tagged proteins were incubated with anti-Myc antibodies for 30 min at 4°C. Following the addition of protein G-Sepharose (GE Healthcare), the mixture was incubated for 16 h at 4°C with gentle rotation. Subsequently, the beads were washed with extraction buffer, and the immune complexes were eluted with SDS–PAGE sample buffer. After SDS–PAGE, the samples were analyzed by western blotting, as described above.

Immunostaining

Briefly, J774 cells stably expressing Myc-tagged proteins were incubated at 37°C for 10 min in the presence of opsonized Texas Red-conjugated zymosan A (Fujifilm Wako Pure Chemical Industries), as described previously (Sakurai *et al.*, 2018). The cells were washed in PBS and fixed with 100% methanol for 7 min at −20°C. Subsequently, the cells were incubated with 2% bovine serum albumin (BSA)/PBS for 30 min at 25°C, treated with anti-Myc antibodies, and stained with goat antimouse IgG antibodies conjugated to Alexa 488 (Thermo Fisher Scientific, Waltham, MA). Images were obtained using an LSM780 confocal laser-scanning microscope with a Plan-Apochromat 63 × /1.40 oil DIC M27 objective lens (Carl-Zeiss, Oberkochen, Germany).

Analysis of phagocytosis with opsonized Texas Red-conjugated zymosan particles

The opsonized Texas Red-conjugated zymosan assay was performed as previously described (Hatsuzawa *et al.*, 2009; Sakurai *et al.*, 2012). Briefly, J774 cells stably expressing Myc-tagged proteins or transfected with siRNAs were incubated for 1 h in the presence or absence of an ~30-fold excess amount of the opsonized Texas Red-conjugated zymosan particles. Subsequently, cells were washed with PBS to remove the free particles and then incubated with 0.025% trypan blue to quench the fluorescence of noninternalized particles. Cellular fluorescence was quantified using an EnSight multimode plate reader (PerkinElmer, Waltham, MA) at an excitation wavelength of 595 nm and emission wavelength of

612 nm. Arbitrary fluorescence units were calculated by subtracting the fluorescence intensity observed in the absence of the zymosan particles from that observed in their presence. Alternatively, for analysis of association efficiency, cells were incubated for 30 min on ice with the particles and then washed thoroughly with PBS to remove the free particles. The fluorescence of particles associated with the cells was then measured, as described previously in this section.

Phagosome-lysosome fusion assay

The phagosome-lysosome fusion assay was performed as described previously (Sakurai *et al.*, 2012). Briefly, J774 cells stably expressing Myc-tagged proteins or transfected with siRNAs were plated onto the center of glass-bottom dishes (35 mm in diameter) and labeled overnight at 37°C with 50 µg/ml RB-dextran (MW 10,000 Da; Invitrogen, Carlsbad, CA). The labeling medium was then removed, and cells were chased for 4 h, washed in ice-cold Hanks' balanced salt solution (HBSS), and incubated first for 30 min on ice in the presence of an ~20-fold excess amount of IgG-opsonized latex beads (3.0 µm in diameter) and then at 30°C for 5 min to initiate phagocytosis. Subsequently, cells were washed three times with ice-cold HBSS and then incubated for 20 min on ice in the presence of Alexa Fluor 488-conjugated goat antirabbit secondary antibodies (Thermo Fisher Scientific). The objective was to stain the beads outside the cells to distinguish them from engulfed beads. Subsequently, the cells were washed with HBSS containing cytochalasin B (at a final concentration of 20 µM, Fujifilm Wako Pure Chemical Industries) for 15 min at 30°C to inhibit the formation of new phagosomes. In Supplemental Figure S7B, cells were cultured with dimethyl sulfoxide (DMSO) or Pitstop 2 (final concentration 30 µM; Sigma-Aldrich). Images were captured using an LSM780 confocal laser-scanning microscope under low-temperature conditions (~6°C). More than 30 phagosomes were counted for each experiment and categorized as RB-dextran-positive or unlabeled phagosomes based on the presence or absence of a detectable RB fluorescence signal. To estimate the amount of RB-dextran-positive organelle, the cells stained with RB-dextran overnight were washed in HBSS. Then, the fluorescence intensity from the cells was quantified in an Infinite F500 multi-mode plate reader (TECAN, Kawasaki, Japan) at an excitation wavelength of 535 nm and an emission wavelength of 612 nm.

Quantification of Myc-positive phagosomes

Latex beads were washed in PBS and incubated with anti-EGFP antibodies for 16 h at 25°C with gentle rotation. The beads were washed in PBS and incubated in 1.5 mg/ml purified TagGFP2 solution for 1 h at 25°C with gentle rotation under light-shielding conditions. The TagGFP2-bound beads were washed in PBS and incubated with anti-EGFP antibodies at 37°C for 1 h. Opsonized TagGFP2-bound beads were washed three times and resuspended in HBSS. J774 cells stably expressing Myc-tagged proteins were washed in HBSS and incubated at 37°C for 1 h in the presence of an ~20-fold excess amount of IgG-opsonized TagGFP2-bound beads. The cells were washed three times in ice-cold HBSS and incubated for 20 min on ice in the presence of Alexa Fluor 647-conjugated donkey antirabbit secondary antibodies (Abcam, Cambridge, UK) to stain the beads outside the cells and distinguish them from engulfed beads. Following incubation, the cells were washed in PBS, and fixed with 100% methanol for 7 min at –20°C. Subsequently, the cells were incubated with 2% BSA/PBS for 30 min at 25°C, treated with anti-Myc antibodies, and stained with goat antimouse IgG antibodies conjugated to Alexa 555 (Thermo Fisher Scientific). Images were obtained using an LSM780 microscope. More than 150 phagosomes were counted for each experiment and categorized into two types (bright or dim beads) based on the presence or absence of TagGFP2 fluorescence signal. The two phagosome types were further classified into two types (Myc-positive phagosome or unlabeled phagosome) based on the presence or absence of detectable Alexa Fluor 555 fluorescence signals.

Quantification of VAMP5- or LAMP1-positive phagosomes

J774 cells stably expressing Myc-tagged proteins were washed in ice-cold HBSS and incubated for 30 min on ice in the presence of an ~20-fold excess amount of IgG-opsonized latex beads incubated for 5 min at 30°C to initiate phagocytosis. The cells were washed three times in ice-cold HBSS and incubated for 20 min on ice in the presence of Alexa Fluor 647 to stain the beads outside the cells to distinguish them from engulfed beads. The cells were then washed in ice-cold HBSS and incubated in HBSS containing DMSO, dynasore (final 50 µM, Enzo Life Sciences, Farmingdale, NY), MiTMAB (final 20 µM, Sigma-Aldrich), or Pitstop 2 for the indicated times at 30°C in the presence of cytochalasin B to inhibit the formation of new phagosomes. Following incubation, the cells were washed in PBS and fixed with 100% methanol for 7 min at –20°C. Subsequently, the cells were incubated with 2% BSA/PBS for 30 min at 25°C, treated with anti-Myc and anti-LAMP1 antibodies, and stained with Alexa Fluor 488-conjugated goat antimouse and Alexa Fluor 594-conjugated goat antirat secondary antibodies (Invitrogen), respectively. Images were captured on an LSM780 microscope. More than 30 phagosomes were counted for each experiment and categorized into two types (Myc- or LAMP1-positive phagosome or unlabeled phagosome) based on the presence or absence of a detectable Alexa Fluor fluorescence signal.

Quantification of clathrin light chain- or dynamin 2-positive phagosomes

Using total RNA extracted from J774 cells, clathrin light chain and dynamin 2 cDNA were obtained by reverse transcription-PCR and confirmed by DNA sequencing. cDNA was cloned into the pmVenus-C1 or pmScarlet-C1 vectors. J774 cells stably expressing Myc-tagged proteins were transiently cotransfected with plasmids of mV-CLC and mSc-Dyn2 using the X-tremeGENE HP DNA Transfection Reagent (Roche Diagnostics, Reinach, Switzerland) according to the manufacturer's instructions. Sixteen hours after transfection, cells were washed in ice-cold HBSS and incubated for 30 min on ice in the presence of an ~20-fold excess amount of IgG-opsonized latex beads, followed by incubation for 5 min at 30°C to initiate phagocytosis. The cells were then washed in ice-cold HBSS and then incubated for 30 min at 30°C in HBSS containing DMSO, dynasore, or MiTMAB in the presence of cytochalasin B, which inhibits the formation of new phagosomes. Images were obtained using an LSM900 microscope. More than 30 phagosomes were counted for each experiment and categorized as labeled or unlabeled phagosomes based on the presence or absence of a detectable mVenus or mScarlet fluorescence signal.

FRET probe

The FRET probe for SNAP23 consisted of TagGFP2ΔC11 (1-227), which lacked C-terminal residues from the pTagGFP2 vector, and TagRFP-t (1-237), in which Ser162 of the pTagRFP-N vector was replaced with Thr, as described previously (Sakurai *et al.*, 2012). The methods for constructing of the tG-S1-tR-S2 (TagGFPΔC11 [1-227]-SNAP23 [1-147] TagRFP-t [1-237] -SNAP23 [148-211]) probe have been described previously (Sakurai *et al.*, 2012).

FRET analysis

The FRET probe of SNAP23 was expressed in J774 cells, stably expressing Myc-tagged proteins using X-tremeGENE HP DNA Transfection Reagent according to the manufacturer's instructions. Fluorescence spectra of probes on the plasma membranes of living cells were obtained 16 h after transfection using an LSM780 confocal laser-scanning microscope at an excitation wavelength of 458 nm. Before measurements, the dynamic range at each wavelength was calibrated using a standard solution according to the manufacturer's instructions. The spectrum analysis with a fluorescence intensity of ~3000 arbitrary units at 503 nm was performed using the LSM780 microscope. FRET efficiency is represented as the 583/503-nm emission ratio. For the phagosomal membrane, 16 h after transfection, the cells were incubated for 30 min on ice, in the presence of an ~50-fold excess of IgG-opsonized zymosan, incubated at 37°C for 5 min to initiate phagocytosis. Subsequently, the cells were washed in ice-cold HBSS, followed by the addition of Pitstop 2 and incubation for 30 min at 37°C in the presence of cytochalasin B to inhibit the formation of new phagosomes. The fluorescence spectra of the probes on the phagosomal membranes were measured as described in this section previously.

Statistical analysis

Data are presented as mean ± standard error of the mean (SEM). Differences between the groups were analyzed by two-tailed, unpaired *t* test or by one-way or two-way analysis of variance (ANOVA) with Tukey's post hoc test using GraphPad Prism 10 (GraphPad Software, San Diego, CA). Statistical significance was defined as $p < 0.05$.

ACKNOWLEDGMENTS

We want to thank Kengo Mekata and Shin Kawano for their technical assistance. We thank all members of our laboratories for their valuable contributions. This work was partly performed at the Tottori Bio Frontier managed by the Tottori prefecture and supported in part by grants from the Japan Society for the Promotion of Science KAKENHI (#JP19K16519 to C.S. and #JP20K06641 to K.H.) and by a grant from the Takeda Science Foundation to C.S. We thank Editage (www.editage.jp) for their help with English language editing.

REFERENCES

Akagi T, Sasai K, Hanafusa H (2003). Refractory nature of normal human diploid fibroblasts with respect to oncogene-mediated transformation. Proc Natl Acad Sci USA 100, 13567–13572.

Bajno L, Peng XR, Schreiber AD, Moore HP, Trimble WS, Grinstein S (2000). Focal exocytosis of VAMP3-containing vesicles at sites of phagosome formation. J Cell Biol 149, 697–706.

Boulais J, Trost M, Landry CR, Dieckmann R, Levy ED, Soldati T, Michnick SW, Thibault P, Desjardins M (2010). Molecular characterization of the evolution of phagosomes. Mol Syst Biol 6, 423.

Braun V, Fraisier V, Raposo G, Hurbain I, Sibarita JB, Chavrier P, Galli T, Niedergang F (2004). TI-VAMP/VAMP7 is required for optimal phagocytosis of opsonised particles in macrophages. EMBO J 23, 4166–4176.

Chen D, Jian Y, Liu X, Zhang Y, Liang J, Qi X, Du H, Zou W, Chen L, Chai Y, *et al.* (2013). Clathrin and AP2 are required for phagocytic receptor-mediated apoptotic cell clearance in *Caenorhabditis elegans.* PLoS Genet 9, e1003517.

Chudakov DM, Matz MV, Lukyanov S, Lukyanov KA (2010). Fluorescent proteins and their applications in imaging living cells and tissues. Physiol Rev 90, 1103–1163.

Dingjan I, Linders PT, Verboogen DRJ, Revelo NH, Ter Beest M, van den Bogaart G (2018). Endosomal and Phagosomal SNAREs. Physiol Rev 98, 1465–1492.

Fairn GD, Grinstein S (2012). How nascent phagosomes mature to become phagolysosomes. Trends Immunol 33, 397–405.

Fasshauer D, Eliason WK, Brunger AT, Jahn R (1998). Identification of a minimal core of the synaptic SNARE complex sufficient for reversible assembly and disassembly. Biochemistry 37, 10354–10362.

Fazeli G, Levin-Konigsberg R, Bassik MC, Stigloher C, Wehman AM (2023). A BORC-dependent molecular pathway for vesiculation of cell corpse phagolysosomes. Curr Biol 33, 607–621.

Fountain A, Inpanathan S, Alves P, Verdawala MB, Botelho RJ (2021). Phagosome maturation in macrophages: Eat, digest, adapt, and repeat. Adv Biol Regul 82, 100832.

Gold ES, Underhill DM, Morrissette NS, Guo J, McNiven MA, Aderem A (1999). Dynamin 2 is required for phagocytosis in macrophages. J Exp Med 190, 1849–1856.

Gopaldass N, Patel D, Kratzke R, Dieckmann R, Hausherr S, Hagedorn M, Monroy R, Kruger J, Neuhaus EM, Hoffmann E, *et al.* (2012). Dynamin A, Myosin IB and Abp1 couple phagosome maturation to F-actin binding. Traffic 13, 120–130.

Hatsuzawa K, Hashimoto H, Hashimoto H, Arai S, Tamura T, Higa-Nishiyama A, Wada I (2009). Sec22b is a negative regulator of phagocytosis in macrophages. Mol Biol Cell 20, 4435–4443.

Hasan N, Corbin D, Hu C (2010). Fusogenic pairings of vesicle-associated membrane proteins (VAMPs) and plasma membrane t-SNAREs – VAMP5 as the exception. PLoS ONE 5, e14238.

Hatsuzawa K, Sakurai C (2020). Regulatory Mechanism of SNAP23 in Phagosome Formation and Maturation. Yonago Acta Med 63, 135–145.

Hong W, Lev S (2014). Tethering the assembly of SNARE complexes. Trends Cell Biol 24, 35–43.

Ikezawa M, Tajika Y, Ueno H, Murakami T, Inoue N, Yorifuji H (2018). Loss of VAMP5 in mice results in duplication of the ureter and insufficient expansion of the lung. Dev Dyn 247, 754–762.

Jahn R, Scheller RH (2006). SNAREs–engines for membrane fusion. Nat Rev Mol Cell Biol 7, 631–643.

Kinchen JM, Doukoumetzidis K, Almendinger J, Stergiou L, Tosello-Trampont A, Sifri CD, Hengartner MO, Ravichandran KS (2008). A pathway for phagosome maturation during engulfment of apoptotic cells. Nat Cell Biol 10, 556–566.

Lancaster CE, Fountain A, Dayam RM, Somerville E, Sheth J, Jacobelli V, Somerville A, Terebiznik MR, Botelho RJ (2021). Phagosome resolution regenerates lysosomes and maintains the degradative capacity in phagocytes. J Cell Biol 220, e202005072

Lee SH, Liu L, Wang YT, Sheng M (2002). Clathrin adaptor AP2 and NSF interact with overlapping sites of GluR2 and play distinct roles in AMPA receptor trafficking and hippocampal LTD. Neuron 36, 661–674.

Levin-Konigsberg R, Mantegazza AR (2021). A guide to measuring phagosomal dynamics. FEBS J 288, 1412–1433.

Levin R, Grinstein S, Canton J (2016). The life cycle of phagosomes: formation, maturation, and resolution. Immunol Rev 273, 156–179.

Macia E, Ehrlich M, Massol R, Boucrot E, Brunner C, Kirchhausen T (2006). Dynasore, a cell-permeable inhibitor of dynamin. Dev Cell 10, 839–850.

Marie-Anais F, Mazzolini J, Herit F, Niedergang F (2016). Dynamin-Actin Cross Talk Contributes to Phagosome Formation and Closure. Traffic 17, 487–499.

Murray RZ, Kay JG, Sangermani DG, Stow JL (2005). A role for the phagosome in cytokine secretion. Science 310, 1492–1495.

Nair-Gupta P, Baccarini A, Tung N, Seyffer F, Florey O, Huang Y, Banerjee M, Overholtzer M, Roche PA, Tampe R, *et al.* (2014). TLR signals induce phagosomal MHC-I delivery from the endosomal recycling compartment to allow cross-presentation. Cell 158, 506–521.

Nguyen JA, Yates RM (2021). Better Together: Current Insights Into Phagosome-Lysosome Fusion. Front Immunol 12, 636078.

Ohno H, Stewart J, Fournier MC, Bosshart H, Rhee I, Miyatake S, Saito T, Gallusser A, Kirchhausen T, Bonifacino JS (1995). Interaction of tyrosine-based sorting signals with clathrin-associated proteins. Science 269, 1872–1875.

Okumura AJ, Hatsuzawa K, Tamura T, Nagaya H, Saeki K, Okumura F, Nagao K, Nishikawa M, Yoshimura A, Wada I (2006). Involvement of a novel Q-SNARE, D12, in quality control of the endomembrane system. J Biol Chem 281, 4495–4506.

Pauwels AM, Trost M, Beyaert R, Hoffmann E (2017). Patterns, receptors, and signals: regulation of phagosome maturation. Trends Immunol 38, 407–422.

Preta G, Cronin JG, Sheldon IM (2015). Dynasore – not just a dynamin inhibitor. Cell Commun Signal 13, 24.

Quan A, McGeachie AB, Keating DJ, van Dam EM, Rusak J, Chau N, Malladi CS, Chen C, McCluskey A, Cousin MA, *et al.* (2007). Myristyl trimethyl ammonium bromide and octadecyl trimethyl ammonium bromide are surface-active small molecule dynamin inhibitors that block endocytosis mediated by dynamin I or dynamin II. Mol Pharmacol 72, 1425–1439.

Sakurai C, Hashimoto H, Nakanishi H, Arai S, Wada Y, Sun-Wada GH, Wada I, Hatsuzawa K (2012). SNAP-23 regulates phagosome formation and maturation in macrophages. Mol Biol Cell 23, 4849–4863.
Sakurai C, Itakura M, Kinoshita D, Arai S, Hashimoto H, Wada I, Hatsuzawa K (2018). Phosphorylation of SNAP-23 at Ser95 causes a structural alteration and negatively regulates Fc receptor-mediated phagosome formation and maturation in macrophages. Mol Biol Cell 29, 1753–1762.
Steel GJ, Tagaya M, Woodman PG (1996). Association of the fusion protein NSF with clathrin-coated vesicle membranes. EMBO J 15, 745–752.
Stow JL, Manderson AP, Murray RZ (2006). SNAREing immunity: the role of SNAREs in the immune system. Nat Rev Immunol 6, 919–929.
Takahashi M, Tajika Y, Khairani AF, Ueno H, Murakami T, Yorifuji H (2013). The localization of VAMP5 in skeletal and cardiac muscle. Histochem Cell Biol 139, 573–582.
Tse SM, Furuya W, Gold E, Schreiber AD, Sandvig K, Inman RD, Grinstein S (2003). Differential role of actin, clathrin, and dynamin in Fc gamma receptor-mediated endocytosis and phagocytosis. J Biol Chem 278, 3331–3338.
Underhill DM, Goodridge HS (2012). Information processing during phagocytosis. Nat Rev Immunol 12, 492–502.
von Kleist L, Stahlschmidt W, Bulut H, Gromova K, Puchkov D, Robertson MJ, MacGregor KA, Tomilin N, Pechstein A, Chau N, *et al.* (2011). Role of the clathrin terminal domain in regulating coated pit dynamics revealed by small molecule inhibition. Cell 146, 471–484.
Weber T, Parlati F, McNew JA, Johnston RJ, Westermann B, Sollner TH, Rothman JE (2000). SNAREpins are functionally resistant to disruption by NSF and alphaSNAP. J Cell Biol 149, 1063–1072.
Zeng Q, Subramaniam VN, Wong SH, Tang BL, Parton RG, Rea S, James DE, Hong W (1998). A novel synaptobrevin/VAMP homologous protein (VAMP5) is increased during in vitro myogenesis and present in the plasma membrane. Mol Biol Cell 9, 2423–2437.